

# Formation of Porous Aggregations Composed of Al<sub>2</sub>O<sub>3</sub> Platelets Using Potassium Sulfate Flux

Shinobu Hashimoto\* and Akira Yamaguchi

Department of Materials Science and Engineering, Nagoya Institute of Technology, Gokiso-cho, Showa-ku, Nagoya 466-8555, Japan

(Received 26 April 1998; accepted 11 August 1998)

## Abstract

*Porous aggregations, with about 10 μm diameter, composed of Al<sub>2</sub>O<sub>3</sub> platelet crystals were formed by heating a powder mixture consisting of Al<sub>2</sub>(SO<sub>4</sub>)<sub>3</sub> + 2K<sub>2</sub>SO<sub>4</sub> (mol ratio) in an alumina crucible at temperatures 1000–1300°C for 3 h and removing the flux component with hot hydrochloric acid after heating. The specific surface area of the aggregations obtained by heating at 1000°C for 3 h was maximum and its value was 5.2 m<sup>2</sup> g<sup>-1</sup>. Since the size of Al<sub>2</sub>O<sub>3</sub> platelets increased and the number of Al<sub>2</sub>O<sub>3</sub> platelets decreased, the specific surface area decreased to 0.7 m<sup>2</sup> g<sup>-1</sup> at 1100°C. When heated at 1300°C, the size of the Al<sub>2</sub>O<sub>3</sub> platelets increased with increasing amount of K<sub>2</sub>SO<sub>4</sub> in the starting powder mixture. © 1999 Elsevier Science Limited. All rights reserved*

**Keywords:** flux growth, platelets, Al<sub>2</sub>O<sub>3</sub>, micro-structure – final, surfaces.

## 1 Introduction

Highly developed anisotropic ceramic particles, for example whiskers and platelets, are used as reinforcements of metal or ceramics to improve their mechanical properties such as elastic modulus, toughness and strength. The use of ceramic whiskers, however, causes difficulties of processing. On the other hand, ceramic platelets are easy to disperse into a matrix phase, and their use has recently increased. Al<sub>2</sub>O<sub>3</sub> platelets have been grown by hydrothermal reaction<sup>1</sup> and in different kinds of fluoride flux.<sup>2,3</sup> Different matrices for example mullite,<sup>4</sup> sialon,<sup>5</sup> aluminium-based metal matrix,<sup>6</sup> glass,<sup>7</sup> (Ce–ZrO<sub>2</sub> + Al<sub>2</sub>O<sub>3</sub>)<sup>8</sup> and TiO<sub>2</sub><sup>9</sup> reinforced by Al<sub>2</sub>O<sub>3</sub> platelets have shown remarkable improvements of the mechanical properties as compared with the unreinforced matrices.

\*To whom correspondence should be addressed.

As a basic research on the formation of porous aggregations composed of Al<sub>2</sub>O<sub>3</sub> platelets with high potential capacity, we have studied the Al<sub>2</sub>O<sub>3</sub> products which are grown by heating Al<sub>2</sub>(SO<sub>4</sub>)<sub>3</sub> in a K<sub>2</sub>SO<sub>4</sub> flux. The aim of this study is to determine the formation temperature of the porous aggregations composed of Al<sub>2</sub>O<sub>3</sub> platelet crystals in the case of heating Al<sub>2</sub>(SO<sub>4</sub>)<sub>3</sub> in K<sub>2</sub>SO<sub>4</sub> flux, to observe the morphology of the Al<sub>2</sub>O<sub>3</sub> and to examine the specific surface area of the Al<sub>2</sub>O<sub>3</sub>. The growth mechanism of the Al<sub>2</sub>O<sub>3</sub> is also discussed.

## 2 Experimental Procedure

As starting materials, Al<sub>2</sub>(SO<sub>4</sub>)<sub>3</sub>·14–18H<sub>2</sub>O and K<sub>2</sub>SO<sub>4</sub> of reagent-grade were used. The Al<sub>2</sub>(SO<sub>4</sub>)<sub>3</sub>·14–18H<sub>2</sub>O was preheated at 300°C for 12 h to form Al<sub>2</sub>(SO<sub>4</sub>)<sub>3</sub>, the formation of which was confirmed by X-ray diffractometry (XRD) analysis. Each powder mixture (about 10 g) consisting of Al<sub>2</sub>(SO<sub>4</sub>)<sub>3</sub>/K<sub>2</sub>SO<sub>4</sub> = 1/1, 1/2 and 1/3 (mol ratio) was put into an alumina crucible (60 mm diameter, 75 mm high) covered by an alumina lid and then heated at temperatures in the range 800–1500°C for 3 h. The heating and cooling rates of the furnace were 10°C min<sup>-1</sup>. After the heat treatment, a mass remained at the bottom of the alumina crucible. The mass was treated with 70–80°C, 1 N hydrochloric acid for 0.5–1 h. White powders were obtained as final products. The powders were analyzed by XRD to identify the crystal phases and the particle morphology of the powders was observed by scanning electron microscopy (SEM). The specific surface area of the powders was examined by the BET method. To elucidate the growth mechanism of this Al<sub>2</sub>O<sub>3</sub>, differential thermal analysis (DTA) and thermogravimetric analysis (TG) for the starting powder mixture were performed up to 800°C with a heating rate of 10°C min<sup>-1</sup>.

### 3 Results and discussion

#### 3.1 Formation

Figure 1 shows XRD patterns of the final powders after heating the powder mixture of  $\text{Al}_2(\text{SO}_4)_3/\text{K}_2\text{SO}_4=1/2$  at various temperatures for 3 h and treating with hot hydrochloric acid. As heated at  $800^\circ\text{C}$ , the powder was identified as  $\text{KAl}(\text{SO}_4)_2$  crystals.  $\text{Al}_2\text{O}_3$  crystals were first detected after heating at temperatures above  $900^\circ\text{C}$ , but the peaks of  $\beta\text{-Al}_2\text{O}_3$  ( $\text{KAl}_5\text{O}_8$  and  $\text{K}_2\text{Al}_{22}\text{O}_{34}$  crystals) were detected in addition at  $1400^\circ\text{C}$ . In the case of heating at  $1500^\circ\text{C}$ , the intensities of the main peaks corresponded to  $\beta\text{-Al}_2\text{O}_3$  ( $\text{KAl}_5\text{O}_8$  and  $\text{K}_2\text{Al}_{22}\text{O}_{34}$ ) and the  $\text{Al}_2\text{O}_3$  signal was very low. That is to say,  $\text{Al}_2\text{O}_3$  powder as a simple crystal phase was obtained at temperatures between  $900$  and  $1300^\circ\text{C}$ . Figure 2 shows SEM photographs of  $\text{Al}_2\text{O}_3$  powder obtained by heating the powder mixture of  $\text{Al}_2(\text{SO}_4)_3/\text{K}_2\text{SO}_4=1/2$  at  $900^\circ\text{C}$ . As a whole, the shape of the  $\text{Al}_2\text{O}_3$  is inhomogeneous. However, nearly spherical aggregations with less than  $10\ \mu\text{m}$  diameter could be observed. The surfaces of the aggregations were rough. Figure 3 shows SEM photographs of  $\text{Al}_2\text{O}_3$  powder obtained by heating the powder mixture of  $\text{Al}_2(\text{SO}_4)_3/\text{K}_2\text{SO}_4=1/2$  at  $1000^\circ\text{C}$ . Most of the  $\text{Al}_2\text{O}_3$  comprised nearly spherical porous aggregations, of about  $10\ \mu\text{m}$ , composed of small platelet crystals. The size of the  $\text{Al}_2\text{O}_3$  platelet crystals which appeared at the surface of the aggregations was  $0.2$  to  $0.4\ \mu\text{m}$  short side and  $1$  to  $2\ \mu\text{m}$  long side.

#### 3.2 Changes of morphology and specific surface area

Figure 4 shows the specific surface area of  $\text{Al}_2\text{O}_3$  powders prepared by heating the powder mixture of  $\text{Al}_2(\text{SO}_4)_3/\text{K}_2\text{SO}_4=1/2$  at temperatures between  $900$  and  $1300^\circ\text{C}$ . The maximum was obtained at

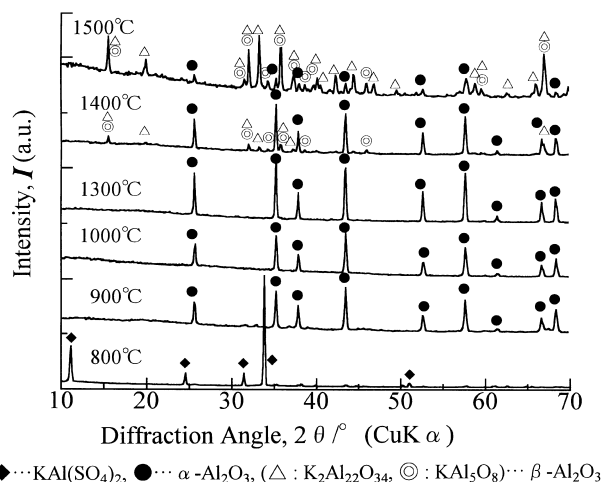


**Fig. 1.** XRD patterns of the final powders after heating the powder mixture of  $\text{Al}_2(\text{SO}_4)_3/\text{K}_2\text{SO}_4=1/2$  at various temperatures for 3 h and treating with hot hydrochloric acid.

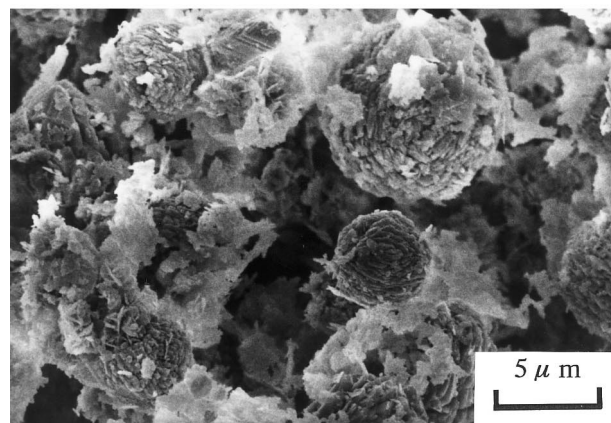
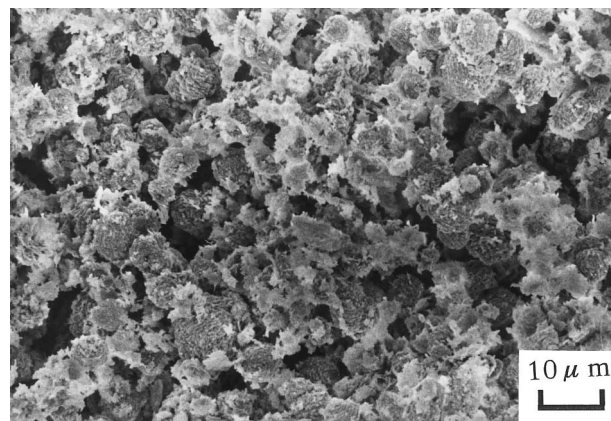


**Fig. 2.** SEM photographs of  $\text{Al}_2\text{O}_3$  powder obtained by heating the powder mixture of  $\text{Al}_2(\text{SO}_4)_3/\text{K}_2\text{SO}_4=1/2$  at  $900^\circ\text{C}$  for 3 h.

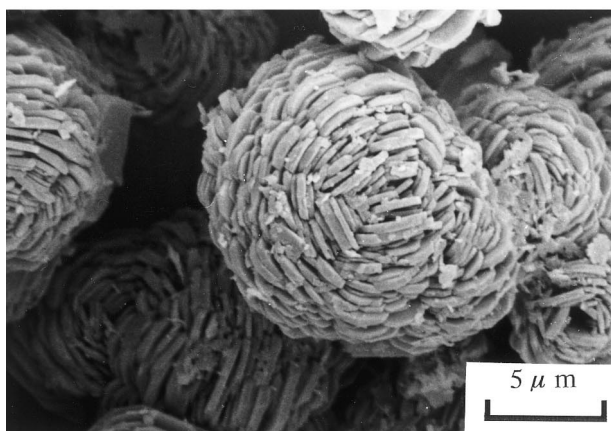
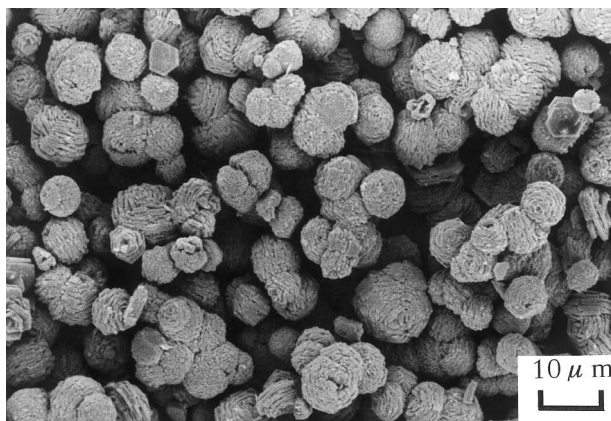


**Fig. 3.** SEM photographs of  $\text{Al}_2\text{O}_3$  powder obtained by heating the powder mixture of  $\text{Al}_2(\text{SO}_4)_3/\text{K}_2\text{SO}_4=1/2$  at  $1000^\circ\text{C}$  for 3 h.

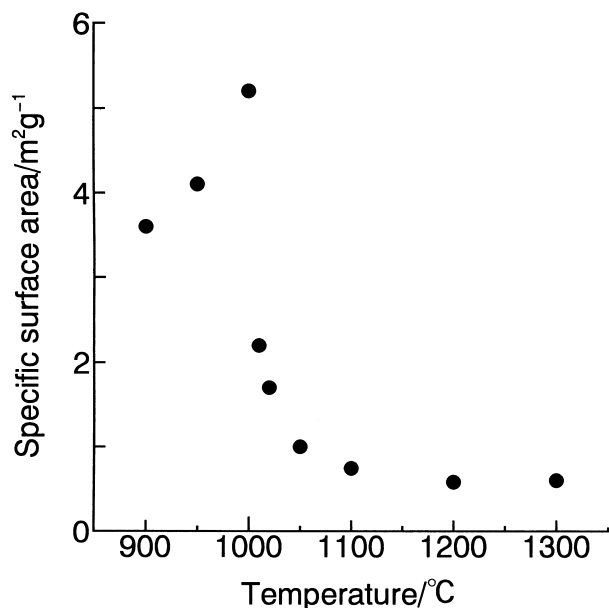


Fig. 4. Specific surface area of  $\text{Al}_2\text{O}_3$  powders prepared by heating the powder mixture of  $\text{Al}_2(\text{SO}_4)_3/\text{K}_2\text{SO}_4 = 1/2$  at temperatures between 900–1300°C for 3 h.

1000°C and its value was  $5.2 \text{ m}^2 \text{ g}^{-1}$ . The specific surface area then decreased to  $0.7 \text{ m}^2 \text{ g}^{-1}$  at 1100°C, keeping almost the same value to 1300°C. Figure 5 shows SEM photographs of  $\text{Al}_2\text{O}_3$  powder obtained by heating the powder mixture of  $\text{Al}_2(\text{SO}_4)_3/\text{K}_2\text{SO}_4 = 1/2$  at 1300°C. Porous aggregations composed of  $\text{Al}_2\text{O}_3$  platelets were again observed. The size of the aggregations was about  $10 \mu\text{m}$  diameter and similar to those shown in Fig. 3. However, the size of the  $\text{Al}_2\text{O}_3$  platelets increased, while the number of platelets decreased. In appearance, the short side and long side of the  $\text{Al}_2\text{O}_3$  platelets near the surface of the aggregations were  $0.5$  to  $1 \mu\text{m}$  and several  $\mu\text{m}$  to  $10 \mu\text{m}$ , respectively. According to SEM observation, the size and morphology of the aggregations composed of  $\text{Al}_2\text{O}_3$  platelets obtained by heating at temperatures 1100–1200°C were similar to those of the aggregations obtained by heating at 1300°C, seen in Fig. 5.

### 3.3 Growth mechanism

Figure 6 shows TG and DTA curves for the starting powder mixture of  $\text{Al}_2(\text{SO}_4)_3/\text{K}_2\text{SO}_4 = 1/2$  up to 800°C. The melting point of  $\text{K}_2\text{SO}_4$  is 1069°C.<sup>10</sup>  $\text{Al}_2(\text{SO}_4)_3$  is desulfurized in air at above 900°C to form  $\text{Al}_2\text{O}_3$ .<sup>11</sup> Two endothermic peaks and one exothermic peak were detected at about 580°C (point a), 660°C (point c) and 620°C (point b), respectively. The first endothermic peak (a) is considered to be caused by the transformation from the  $\beta$ - (low temperature form) to the  $\alpha$ -phase (high temperature form) of  $\text{K}_2\text{SO}_4$ .<sup>10,12</sup> The powder mixture which was heated to 640°C and then cooled rapidly to room temperature resembled the

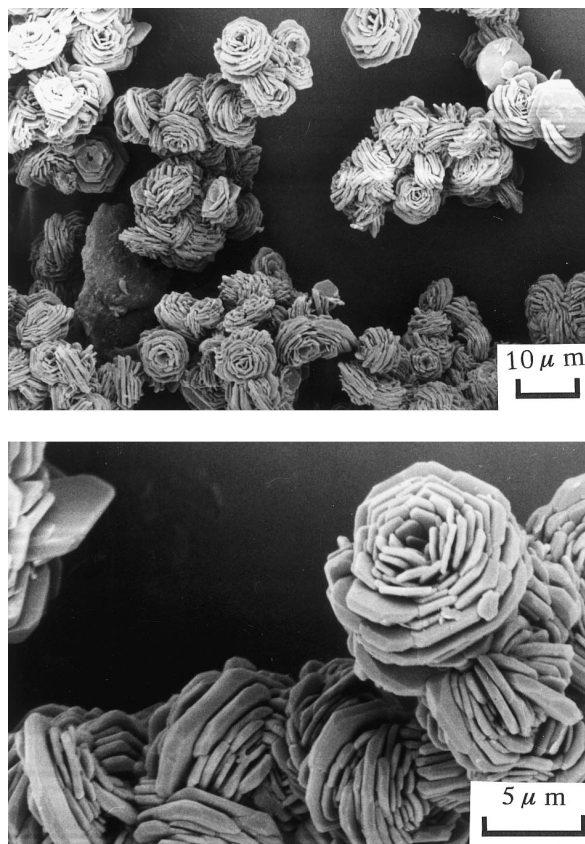


Fig. 5. SEM photographs of  $\text{Al}_2\text{O}_3$  powder obtained by heating the powder mixture of  $\text{Al}_2(\text{SO}_4)_3/\text{K}_2\text{SO}_4 = 1/2$  at 1300°C for 3 h.

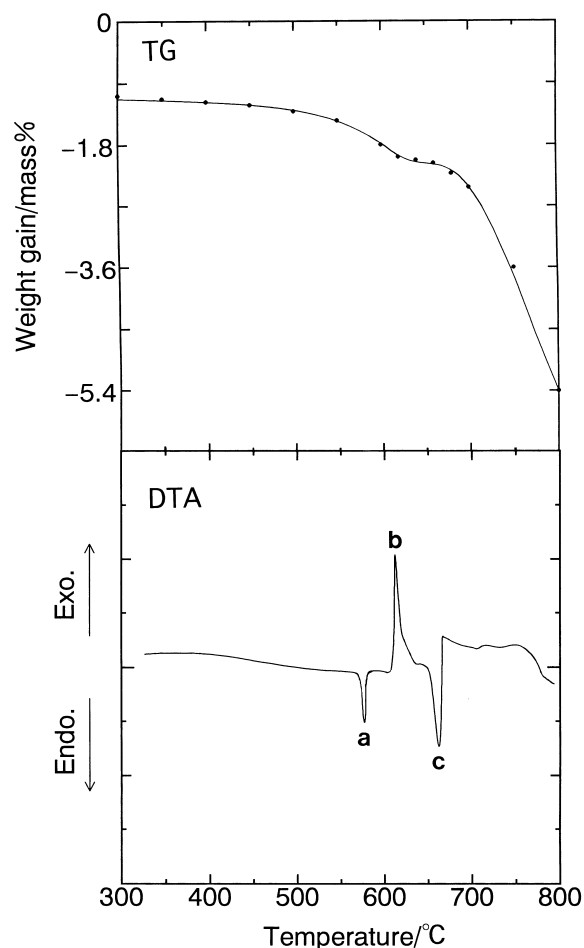


Fig. 6. TG and DTA curves for the starting powder mixture of  $\text{Al}_2(\text{SO}_4)_3/\text{K}_2\text{SO}_4 = 1/2$  up to 800°C.

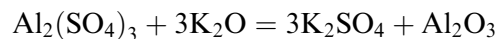
starting powder mixture and was mostly identified as  $K_3Al(SO_4)_3$  crystals, although low intensity peaks corresponding to  $KAl(SO_4)_2$  and  $Al_2(SO_4)_3$  were detected. Therefore, the exothermic (b) is considered to be caused by the formation of  $K_3Al(SO_4)_3$  crystal. Since after the DTA cycle (heated up to  $800^\circ\text{C}$ ) of the starting powder mixture, no individual particles could be distinguished and luster was observed in some places, the second endothermic peak (c) is considered to be due to the formation of a liquid phase.

The reason why the final powder obtained by heating the powder mixture of  $Al_2(SO_4)_3/K_2SO_4 = 1/2$  at  $800^\circ\text{C}$  for 3 h was identified as  $KAl(SO_4)_2$  crystal, as seen in Fig. 1, is that the composition of the liquid changed by the vaporization of  $SO_3$  (g) with heating, which was noticed in the TG curve of Fig. 6; the  $KAl(SO_4)_2$  finally crystallized from the liquid during cooling.

According to SEM observation of the  $Al_2O_3$  powder obtained by rapid cooling to room temperature after heating the powder mixture of  $Al_2(SO_4)_3/K_2SO_4 = 1/2$  at  $1000^\circ\text{C}$  for 3 h, the size and morphology of the porous aggregations of  $Al_2O_3$  platelets were almost the same as those

cooled at  $10^\circ\text{C min}^{-1}$ , seen in Fig. 3. The aggregations composed of  $Al_2O_3$  platelets are considered to be grown in the liquid phase during heating.

Since the change of Gibbs' free energy ( $\Delta G^\circ$ ) for the following equation at  $827^\circ\text{C}$  (1100 K) is  $-1442.114 \text{ kJ mol}^{-1}$ , based on thermochemical data,<sup>10</sup> it is expected that nucleation is caused and that stable  $Al_2O_3$  crystals precipitate in the liquid phase.



With increasing temperature, it is considered that the vaporization of  $SO_3$  (g) from the liquid is accelerated to form  $Al_2O_3$  crystal. As shown in Fig. 7 which shows the formation process of the porous aggregations of  $Al_2O_3$  platelets, during the second stage, multinucleation of  $Al_2O_3$  crystals may occur at the surface of the original  $Al_2O_3$  crystal. They will grow to form the aggregation of  $Al_2O_3$  platelets.

Figures 8 and 9 show SEM photographs of  $Al_2O_3$  powder obtained by heating the powder mixtures of  $Al_2(SO_4)_3/K_2SO_4 = 1/1$  and  $1/3$  at  $1300^\circ\text{C}$  for 3 h, respectively. In the case of heating the powder mixture of  $1/1$ ,  $Al_2O_3$  platelets

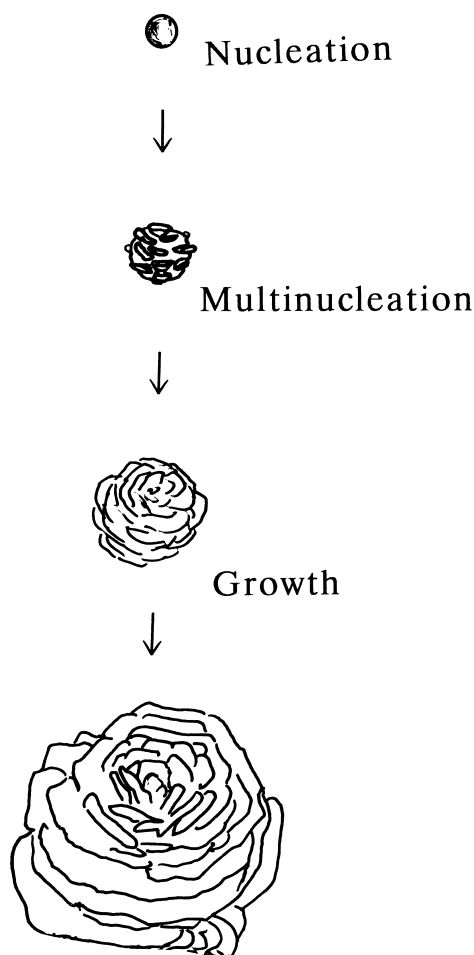


Fig. 7. Schematic drawing for the formation process of the porous aggregations of  $Al_2O_3$  platelets.

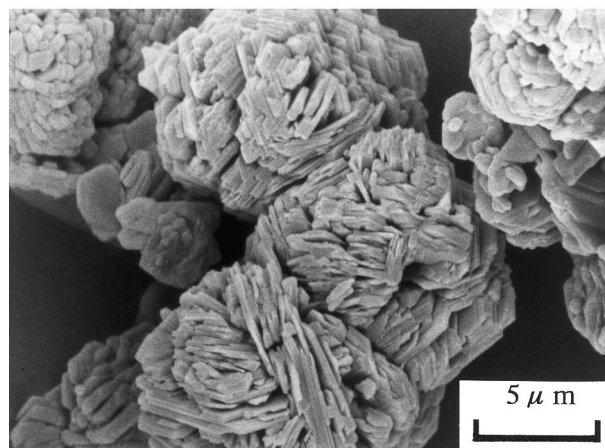
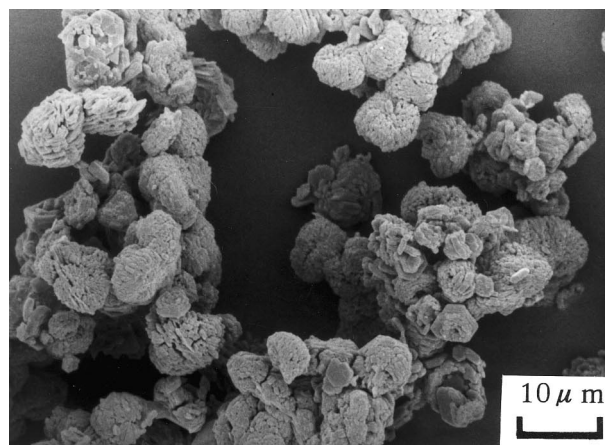
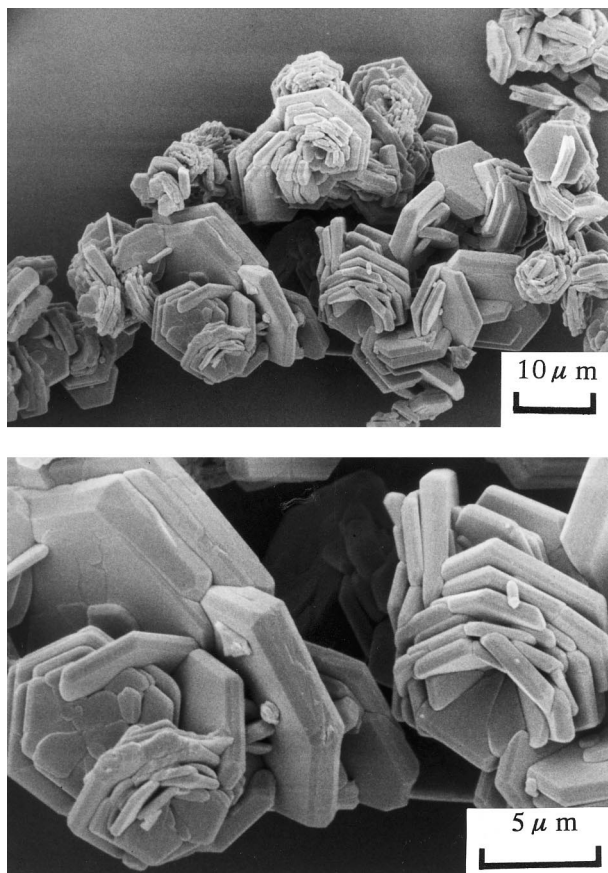


Fig. 8. SEM photographs of  $Al_2O_3$  powder obtained by heating the powder mixture of  $Al_2(SO_4)_3/K_2SO_4 = 1/1$  at  $1300^\circ\text{C}$  for 3 h.



**Fig. 9.** SEM photographs of  $\text{Al}_2\text{O}_3$  powder obtained by heating the powder mixture of  $\text{Al}_2(\text{SO}_4)_3/\text{K}_2\text{SO}_4 = 1/3$  at  $1300^\circ\text{C}$  for 3 h.

appeared to be interlinked to each other due to shortage of the liquid phase during heating. On the other hand, with heating the powder mixture of  $1/3$ ,  $\text{Al}_2\text{O}_3$  platelets grew. The amount of the liquid phase is considered to be enough for the  $\text{Al}_2\text{O}_3$  platelets to develop.  $\text{K}_2\text{SO}_4$  is considered to take an important part as the flux component in this method.

#### 4 Conclusions

To form porous aggregations composed of  $\text{Al}_2\text{O}_3$  platelets, powder mixture consisting of  $\text{Al}_2(\text{SO}_4)_3$  and  $\text{K}_2\text{SO}_4$  were heated at temperatures between  $800$  and  $1500^\circ\text{C}$  and treated with hot hydrochloric acid to remove the flux component after heating. The major results are as follows.

1. On heating the powder mixture of  $\text{Al}_2(\text{SO}_4)_3/\text{K}_2\text{SO}_4 = 1/2$ , porous aggregations, of about  $10\ \mu\text{m}$  diameter, composed of  $\alpha\text{-Al}_2\text{O}_3$  platelet

crystals were obtained by heating at temperatures  $1000\text{--}1300^\circ\text{C}$ . As heated at temperatures  $1100\text{--}1300^\circ\text{C}$ , the size of the  $\text{Al}_2\text{O}_3$  platelets increased and the number of  $\text{Al}_2\text{O}_3$  platelets decreased, as compared with those formed at  $1000^\circ\text{C}$ .

The specific surface area of the aggregations composed of  $\text{Al}_2\text{O}_3$  platelets reached  $5.2\ \text{m}^2\ \text{g}^{-1}$  at  $1000^\circ\text{C}$ , it then decreased to  $0.7\ \text{m}^2\ \text{g}^{-1}$  at  $1100^\circ\text{C}$  and was almost constant for temperatures  $1100\text{--}1300^\circ\text{C}$ .

2. In the case of heating at  $1300^\circ\text{C}$ , the size of the  $\text{Al}_2\text{O}_3$  platelets increased with increasing  $\text{K}_2\text{SO}_4$  in the starting powder mixture.

#### References

1. Chase, A. B. and Osmer, J. A., Habit changes of sapphire grown from  $\text{PbO}\text{--}\text{PbF}_2$  and  $\text{MoO}_3\text{--}\text{PbF}_2$  fluxes. *J. Am. Ceram. Soc.*, 1970, **53**, 343–345.
2. Shaklee, C. A. and Messing, G. L., Growth of  $\alpha\text{-Al}_2\text{O}_3$  platelets in the  $\text{HF}\text{--}\gamma\text{-Al}_2\text{O}_3$  system. *J. Am. Ceram. Soc.*, 1994, **77**, 2977–2984.
3. Ono, S., Yamaguchi, G., Yanagida, H. and Shimizu, T., Effects of impurities on hydrothermal reactions of Alumina. *Yogyo-Kyokai-Shi (Japan)*, 1968, **76**, 207–218.
4. Zhou, Y., Vleugels, J., Laoui, T. and Van Der Biest, O., Toughening of sol-gel derived mullite matrix by  $\text{Al}_2\text{O}_3$  platelets. *J. Mater. Sci. Lett.*, 1994, **13**, 1089–1091.
5. Zhou, Y., Vleugels, J., Laoui, T. and Van Der Biest, O., Toughening of X-Sialon with  $\text{Al}_2\text{O}_3$  platelets. *J. Eur. Ceram. Soc.*, 1995, **15**, 297–305.
6. Massardier, V., Fougères, R. and Merle, P., Comparison between the experimental and theoretical tensile behaviour of aluminium-based metal matrix composites reinforced with preforms of  $\alpha$ -alumina platelets. *Mater. Sci. Eng.*, 1995, **A203**, 93–104.
7. Kageyama, K., Enoki, M. and Kishi, T., Mechanical properties of alumina particles and platelet-reinforced glass composites with a crystalline phase at the interface. *J. Ceram. Soc. Japan*, 1995, **103**, 205–210.
8. Roeder, R. K., Trumble, K. P. and Bowman, K. J., Microstructure development in  $\text{Al}_2\text{O}_3$ -platelet-reinforced  $\text{Ce}\text{--}\text{ZrO}_2/\text{Al}_2\text{O}_3$  composites. *J. Am. Ceram. Soc.*, 1997, **80**, 27–36.
9. Fredel, M. C. and Boccaccini, A. R., Processing and mechanical properties of biocompatible  $\text{Al}_2\text{O}_3$  platelet-reinforced  $\text{TiO}_2$ . *J. Mater. Sci.*, 1996, **31**, 4375–4380.
10. Brain, I., *Thermochemical Data of Pure Substance, Part I, Ag–Kr*, 2nd edn, ed. G. Schulz and P. Ryan-Bugler. VHC, Weinheim, Germany, 1993, p. 923.
11. Kato, E., Dimon, K., Yamaguchi, A. and Yamada, T., Sinterability of alumina powders prepared in different processes from hydrated sulfate. *Yogyo-Kyokai-Shi (Japan)*, 1977, **85**, 134–140.
12. Pannetier, G. and Gaultier, M. Analyse radiocristallographique des formes basse ( $\beta$ ) et haute ( $\alpha$ ) temperature des sulfates de potassium et de thallium (I). *Bull. Soc. Chim. France*, 1966, January, 188–194.